J. Membrane Biol. 148, 211–222 (1995)

The Journal of
Membrane
Biology

Excitation-Calcium Release Uncoupling in Aged Single Human Skeletal Muscle Fibers

O. Delbono[1], K.S. O'Rourke[2], W.H. Ettinger[3]

[1]Departments of Physiology and Pharmacology, and Internal Medicine (Gerontology), Bowman Gray School of Medicine, Wake Forest University, Medical Center Boulevard, Winston-Salem, NC 27157

[2]Department of Internal Medicine (Rheumatology), Bowman Gray School of Medicine, Wake Forest University, Medical Center Boulevard, Winston-Salem, NC 27157

[3]Departments of Internal Medicine (Gerontology) and Public Health Sciences, Bowman Gray School of Medicine, Wake Forest University, Medical Center Boulevard, Winston-Salem, NC 27157

Received: 5 May 1995/Revised: 3 August 1995

Abstract. The biological mechanisms underlying decline in muscle power and fatigue with age are not completely understood. The contribution of alterations in the excitation-calcium release coupling in single muscle fibers was explored in this work. Single muscle fibers were voltage-clamped using the double Vaseline gap technique. The samples were obtained by needle biopsy of the *vastus lateralis* (quadriceps) from 9 young (25–35 years; 25.9 ± 9.1; 5 female and 4 male) and 11 old subjects (65–75 years; 70.5 ± 2.3; 6 f, 5 m). Data were obtained from 36 and 39 fibers from young and old subjects, respectively. Subjects included in this study had similar physical activity. Denervated and slow-twitch muscle fibers were excluded from this study. A significant reduction of maximum charge movement (Q_{max}) and DHP-sensitive Ca current were recorded in muscle fibers from the 65–75 group. Q_{max} values were 7.6 ± 0.9 and 3.2 ± 0.3 nC/μF for young and old muscle fibers, respectively ($P < 0.01$). No evidences of charge inactivation or interconversion (charge 1 to charge 2) were found. The peak Ca current was (−)4.7 ± 0.08 and (−)2.15 ± 0.11 μA/μF for young and old fibers, respectively ($P < 0.01$). The peak calcium transient studied with mag-fura-2 (400 μM) was 6.3 ± 0.4 μM and 4.2 ± 0.3 μM for young and old muscle fibers, respectively. Caffeine (0.5 mM) induced potentiation of the peak calcium transient in both groups. The decrease in the voltage-/Ca-dependent Ca release ratio in old fibers (0.18 ± 0.02) compared to young fibers (0.47 ± 0.03) ($P < 0.01$), was recorded in the absence of sarcoplasmic reticulum calcium depletion. These data support a significant reduction of the amount of Ca available for triggering mechanical responses in aged skeletal muscle and, the reduction of Ca release is due to DHPR-ryanodine receptor uncoupling in fast-twitch fibers. These alterations can account, at least partially for the skeletal muscle function impairment associated with aging.

Key words: Dihydropyridine receptor — Muscle contraction — Calcium release — Voltage-clamp — Calcium channels — Muscle weakness

Introduction

Skeletal muscle strength declines with aging as demonstrated in studies on muscle contractility in vivo and in vitro (Edstrom & Larsson, 1987; Brooks & Faulkner, 1988, 1991, 1994; Booth, Weeden, & Tseng, 1993). A central issue regarding the decline of skeletal muscle performance with aging is whether muscle atrophy explains entirely the decrease in contractile properties with aging. Studies on in vitro contractility showed that when the maximum isometric force for aged mice (Brooks et al., 1988; Phillips, Bruce, & Woledge, 1991) and rats (Gutmann & Carlson, 1976; Larsson & Edström, 1986; Fitts et al., 1984) is normalized by the smaller total muscle fiber cross-sectional area, a deficit of 20% in specific isometric force remains unexplained by atrophy (Carlson & Faulkner, 1988; Brooks & Faulkner, 1994*a*). Studies on skinned muscle fibers demonstrated that the force generated per unit cross-sectional area does not differ in adult and old mice during isometric and shortening contractions (Brooks & Faulkner, 1994*b*). These data suggest that other factors in addition to reductions in contractile proteins are contributing to muscle weakness in

Correspondence to: O. Delbono

aged muscles. Since changes in phosphorus metabolites involved in energy transduction (phosphocreatine, ATP, ADP) and percentage of myosin isoforms do not change with aging in muscles composed exclusively of one type of fiber (Phillips et al., 1993), it is likely that earlier steps in excitation-contraction coupling are altered. An incomplete calcium activation can account for differences in normalized tension in adult and aged muscles. A small right shift in calcium sensitivity of the regulatory proteins of the muscle has been reported (Brooks & Faulkner, 1994*b*). However, information about concentrations of these proteins, sarcoplasmic reticulum (SR) calcium content and volume, and sarcolemmal structure in adult and old muscles is incomplete or controversial (Fujisawa, 1975; De Coster et al., 1981).

The mechanisms underlying decline in muscle power and fatigue in the elderly are not known. Several hypothesis have been proposed as to the biological mechanisms underlying muscle impairment with aging. Some of these mechanisms are: selective type II fiber atrophy, muscle denervation-reinnervation and, contraction-induced injury. In some studies, a primary atrophy of type II fibers without alterations in fiber type distribution has been reported, and it had been difficult to attribute these changes to aging or inactivity (Coggan et al., 1992). A selective muscle fiber denervatory and reinnervatory process leads to motor unit remodeling (Campbell, McComas & Petito, 1973; Edstrom & Larsson, 1987; Kanda & Hashizume, 1989; Brooks & Faulkner, 1994*b*), resulting from a net loss of predominantly type II fibers (Lexell et al., 1983; Edstrom & Larsson, 1987). An increased susceptibility to contraction-induced injury associated with impaired capacity for regeneration in aged skeletal muscle has also been reported (Brooks & Faulkner, 1993*b*) as a contributing factor to skeletal muscle impairment with aging.

In this work, we explored potential alterations in the excitation-calcium release process in fast-twitch human skeletal muscle fibers as an underlying mechanism of muscle weakness in old age. Fast-twitch fibers were selected for this study because they depict the most significant degree of hypo-atrophy with aging in mixed fiber-type composition muscles (*see above*). Specifically, this study was designed to test the hypothesis that in addition to already identified determinants of muscle impairment with aging, a reduced function of the dihydropyridine receptor (DHPR) has consequences on excitation-calcium release coupling. DHPRs are involved in triggering calcium release from the sarcoplasmic reticulum (voltage-gated calcium release) playing a fundamental role during brief and prolonged contractions. Calcium influx through DHPRs is relevant for sustained contractions in mammalian fibers (Kotsias, Muchnik & Obejero Paz, 1986; Sculptoreanu, Scheuer & Catterall, 1993). In summary, DHPRs act as voltage-sensors and as ion-conducting pores. Alterations of the DHPR-ryanodine receptor (RYR) coupling or calcium influx can account, at least partially, for decreases in muscle contractility in aged muscles.

Single muscle fibers have been used in this work because this preparation has distinct advantages for studying the mechanisms of excitation-contraction coupling in aged muscles. Some advantages include the preservation of the DHPR-RYR interaction and of the intracellular constituents such as regulatory proteins and calcium buffers. Unfortunately, muscle fibers do not retain their properties in culture, suffering dedifferentiation to a variable extent. Thus, single muscle fibers are an important tool for exploring the role of the sarcolemma and the cytosolic milieu in muscle function at different ages.

Materials and Methods

Subjects Physical Condition

The subjects for this research were community-dwelling volunteers recruited through advertisements. Study subjects met the following criteria: age 25–35 or 65–75, in general good health, independent in all activities of daily life and not participating in a regular exercise program. Potential participants were excluded if they reported a history of cardiovascular, metabolic or musculoskeletal disease, were taking a medication that affects muscle or calcium metabolism, or participated in regular exercise or sport activity defined as greater than 20 min per session more than one time per week. Subjects that received aspirin for 7 days or nonsteroid antiinflammatory drugs or coumadin for 4 days preoperation were excluded. The procedures employed in this study were approved by the Clinical Research Practices Committee of The Bowman Gray School of Medicine of Wake Forest University.

Skeletal Muscle Biopsy

This procedure was performed with the understanding and consent of each individual and the approval of the local Ethics Committee. Needle muscle biopsy of the *vastus lateralis* (quadriceps) was performed with a University College Hospital (UCH) muscle biopsy needle (Bergström, 1962; Larsson & Salviati, 1992) as previously described (O'Rourke, Blaivas & Ike, 1994). Using a sterile technique, local anesthesia was provided with 1% lidocaine. A 5-mm incision parallel to the skin lines was made. The needle was positioned to pierce the skin at an angle of 30–40° to the surface and inserted nearly parallel to the femur with slight medial angulation, penetrating the muscle to a depth sufficient to encompass the entire cutting window of the instrument. A total of 2–4 such biopsies per needle insertion were performed before the needle was withdrawn.

Skeletal Muscle Fiber Preparation

Muscle samples were placed in a beaker containing a modified Krebs solution (*see below*) immediately after their obtainment. A small bundle of fibers was dissected and transferred to a chamber with the dissecting solution. A 0.5–1-cm segment of muscle fiber was isolated in this solution and then transferred to the experimental chamber containing the mounting solution. The chamber and the external surface of the

fiber membrane were divided into three compartments by Vaseline strands. Two seals were formed around the fiber when a coverslip was put over the preparation. After that, the mounting solution was replaced by the extracellular solution in the middle pool and by the intracellular solution in the end pools. Fibers were mounted and stretched to 3.7 μm sarcomere in the experimental chamber to prevent mechanical artifacts during intracellular Ca^{2+} transients measurements.

The data were obtained from 9 young (25–35 years; 25.9 ± 9.1; 5 female and 4 male) and 11 old subjects (65–75 years; 70.5 ± 2.3; 6 f, 5 m).

Electrical Recordings

We used the double Vaseline gap voltage-clamp technique (Francini & Stefani, 1989; Delbono et al., 1991). Briefly, agar bridges equilibrated with the end-pool or middle-pool solutions provided electrical connections between each compartment and separate wells that were filled with 3 M KCl and fitted with an Ag/AgCl pellet. Command pulses referred to ground were applied at the central pool. The current was injected into one of the end pools via a variable gain feedback amplifier. The negative input of the amplifier was connected to the other end pool (E). Membrane potential was measured between the middle pool and compartment E, and the current as the voltage drop across a 100-K resistance. The membrane potential was held at −80 mV in experiments with simultaneous fluorescent determinations or at −90 mV for studies on charge movement distribution in depolarized fibers.

Data Collection

Data were collected on line with a microcomputer. Signals were acquired with a AD/DA Labmaster converter (Axon Instruments, Foster City, CA) and filtered at 0.3 of the sampling frequency (−3 dB point) with a 4-pole Butterworth filter. Linear components of the membrane were digitally subtracted by control pulses—¼ of the amplitude of the test pulse from the holding potential (at −90 or −80 mV, as indicated for each group of experiments). Control pulses were delivered immediately before the test pulse. For fluorescent recordings, the fiber was epi-illuminated with a 75-W xenon lamp. The UV beam passed through selectable 350 or 380 nm excitation wavelength filters mounted in a Ludl filter wheel, with 10-nm bandwidth (Omega Optical, Brattleboro, VT), and was reflected downward by a long pass dichroic mirror centered at 400 nm (DC 400 LP, Omega Optical, Brattleboro, VT) and at a 45° angle. The light beam was focused onto the fiber with a 63× (N.A. 1.3) objective (Zeiss, Germany), which transmitted light without major distortion up to 320 nm. After illuminating the fiber, the upward emitted light beam was collected by the objective and stimulated the photodiode (UDT-455UV, UDT Sensors, Hawthorne, CA) after passing through the long pass dichroic mirror and an emission filter, centered at 510 nm with 40 nm bandwidth. The photodiode current was recorded with a current to voltage converter with 1 gigaohm feedback resistance to improve the signal-to-noise ratio. The frequency response was adjusted to 5 kHz with a high frequency booster using an intermittent light source. The fiber was periodically illuminated during stimulation using a computer-controlled shutter-filter wheel. All the records were corrected for photobleaching. In resting conditions, fiber illumination caused a linear decline of fluorescence with time. In most of our records, the bleaching correction at 6 sec after a 200-msec pulse to 0 mV represented 5% of the signal and about 0.5% of resting fluorescence. For a description of the fluorescent measurements and in vivo and in vitro dye calibrations, *see* Delbono et al. (1993). For calcium concentration calculations, 380/350 nm ratios were used according to described procedures (Grynkiewicz, Poenie & Tsien, 1985).

Solutions

The composition of the solutions is (mM): Modified Ringer: NaCl 145, KCl 5, $CaCl_2$ 2.5, $MgSO_4$ 1, Na-HEPES 10, glucose 10; Dissecting: K_2SO_4 95, $MgCl_2$ 10, $CaCl_2$ 0.4, Na-HEPES 10; Mounting: K-glutamate 150, $MgCl_2$ 2, K_2-EGTA 1, K-HEPES 10; Extracellular: TEA-CH_3SO_3 150, $CaCl_2$ 10, $MgCl_2$ 2, TEA-HEPES 5, 9 anthracenecarboxylic 1, acid tetrodotoxin (TTX) 0.0005; Internal solution: Na-glutamate 98, K_2-EGTA 0.1, $CaCl_2$ 0.0082, Na_2ATP 5, $MgCl_2$ 5.5, glucose 5, K-HEPES 5, Na_2-phosphocreatine 5, ph ≈ 7.2. The osmolarity of the solutions was 300 mOsm. Mag-fura-2 (Molecular Probes, Eugene, OR) was added from 5 mM stock solutions (in deionized water) to final concentrations of 400 μM. Free Ca^{2+} concentrations in solutions were calculated according to Fabiato (1983). Co^{2+} (2 mM) in the external solution was used to abolish calcium current during charge movement recordings. Temperature was monitored with a thermistor probe positioned close to the fiber in the middle pool and kept at 22°C.

Calculation of Ca^{2+} Release

SR calcium release was calculated as described previously (Melzer, Ríos & Schneider, 1986; Brum, Ríos & Stefani, 1988; Delbono & Stefani, 1993). Basically, the rate of Ca^{2+} release is equal to the difference between the input and output fluxes. The input flux corresponds to the Ca^{2+} release, while the output flux to the myoplasmic Ca^{2+} removal system. The voltage-independence of the myoplasmic calcium removal process has been ascertained recently in rat muscle fibers (Delbono & Chu, 1995). Thus, the mathematical algorithm has been found suitable to describe calcium fluxes in mammalian fibers (Delbono & Stefani, 1993; García & Schneider, 1993; Delbono, 1995). The calcium release function shows a fast initial peak and a smaller, more prolonged steady state phase. These two phases represent the calcium- and voltage-gated SR calcium release, respectively (Jacquemond, Kao & Schneider, 1991; Delbono & Chu, 1995). The procedures for operating the model to obtain reliable calcium influx measurements have been described more recently (González & Ríos, 1993). Basically, a computer program fits a set of parameters (Delbono & Stefani, 1993) to the decaying phase of Ca^{2+} transients of different amplitude and durations, using a nonlinear least-squares routine. Once the same set of values fits all the records, the calcium release function is calculated.

Denervation at the Single Fiber Level

Morphological changes induced by denervation have been described (Engel & Stonnington, 1974). Specially important for this study are the procedures to detect muscle fiber denervation under calcium current recording conditions (Delbono, 1992). A new population of Na^+ channels resistant to TTX is expressed in skeletal muscle upon denervation. The activation and inactivation parameters of the new sodium channels are shifted to more negative potentials by approximately 10 mV. Thus, at a holding potential negative to −80 mV, there is a large fraction of Na^+ channels available for opening that can be increased by hyperpolarizing the membrane. Charge movement and I_{Ca} were recorded in the presence of Na^+ as the main intracellular cation. A fast outward current at the beginning of the traces which is not present in the tail current is a test to determine whether this fast outward current passed through Na^+ channels. In some fibers, the intracellular Na^+ was replaced by Cs^+

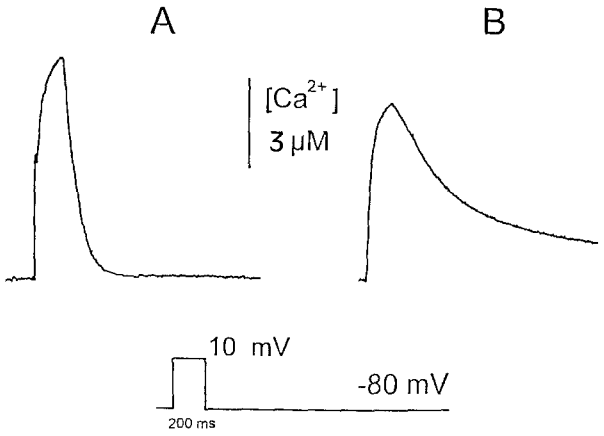

Fig. 1. Calcium transients recorded with 400 μM mag-fura-2 in fast-twitch (*A*) and slow-twitch (*B*) quadriceps fibers in response to 200 msec pulse from $V_h = -80$ to +10 mV. Calcium transients signals are expressed in calcium concentration.

which does not permeate through this channel, resulting in a dramatic decrease in the amplitude of the outward current. Thus, the presence of TTX-resistant Na^+ outward current is an indication of muscle fiber denervation. Fibers with these properties were not included in the present study. Charge movement, and I_{Ca} activation and inactivation in denervated fibers were studied previously (Dulhunty & Gage, 1985; Delbono, 1992). Only 4 fibers from the older group were denervated. No evidences of denervation were detected in young muscle samples.

Identification of Fast- and Slow-twitch Muscle Fibers

The *vastus lateralis* from the human quadriceps muscle has a heterogeneous fiber-type composition. The relative predominance of a fiber subtype is controversial (Johnson et al., 1973; Saltin & Gollnick, 1983). As a predominant atrophy of fast-twitch muscle fibers has been reported in aging (Lexell et al., 1983), we identified the two major fiber types to explore the former more in detail. To this end, calcium transient rates of decay were studied in each fiber. Fast- and slow-twitch muscle fibers differ in calcium transient amplitude, calcium transient rate of decay and myoplasmic parvalbumin, a calcium binding protein. Undetectable concentrations of parvalbumin in slow fibers have been reported (Heizmann, 1984). The lack of parvalbumin is responsible for the slow return to prestimulation myoplasmic $[Ca^{2+}]$ in slow-twitch muscle. In this work, fibers were classified as fast- and slow-twitch type based on: (i) the time constant (τ) of the Ca^{2+} transient decay in response to 200 msec depolarizing pulses from $V_h = -80$ to +10 mV and, (ii) the amount of residual $[Ca^{2+}]$ 200 msec after the end of a pulse with the same amplitude and duration. Typically, Ca^{2+} removal was fitted to a single exponential function in fast-twitch fibers ($\tau = 38.2 \pm 2.3$ msec, *n* fibers = 75) and, to a single exponential function plus a constant in slow-twitch fibers ($\tau = 102.3 \pm 12.2$ msec, n = 5). The residual $[Ca^{2+}]$ was 0 and 46 ± 6% (n = 5) of the peak Ca^{2+} transient for fast- and slow-twitch fibers, respectively, at 200 msec after repolarization. Figure 1 shows calcium transients measured in fast-twitch (*A*) and slow-twitch (*B*) fibers in response to 200-msec pulse from $V_h = -80$ to +10 mV. Note the smaller amplitude and slower decay of Ca^{2+} transients in slow twitch. It has to be noticed that "zero" residual in the former means that $[Ca^{2+}]$ returned to prestimulation concentrations detected with a high K_D Ca^{2+} indicator (mag-fura-2). The use of lower K_D dyes such as fura-2 allows the detection of $[Ca^{2+}]$ above the resting values for several seconds after repolarization in fast-twitch mammalian muscle fibers (Delbono, 1995). In this study, 5 fibers were slow-twitch type, 2 from young and 3 from older muscles. Probably, the major reason for the high fast-fiber proportion in both groups is the smaller amount of connective tissue inside the fast-contracting fascicles, facilitating the dissection.

Results

Throughout this work data result from the analysis of 36 fibers (mean = 4, range = 3 to 5 fibers) from 9 young subjects (25–35 years) and of 39 fibers (mean = 3.8, range = 2 to 5 fibers) from 11 old subjects (65–75 years). Only fibers with kinetic characteristics of the fast-twitch type and without evidence of denervation were included in the present work (*see* Materials and Methods). All the fiber from the aged group included in this study depicted marked hypo-atrophy. The mean fiber diameter in the aged group was significantly smaller than in the younger group (*see* Table).

Charge Movement and I_{Ca} in Aged Skeletal Muscle Fibers

We explored the DHPR function in living skeletal muscle fibers simultaneously with intracellular calcium responses. The amount of charge movement (measurement independent of channel open probability) and the dihydropyridine-sensitive calcium current (measurement dependent on channel open probability) were assessed as an indication of DHPRs amount and function. These determinations were correlated with the amount of SR Ca^{2+} release in each fiber.

Figure 2 shows charge movement traces at different potentials (from −70 to +30 mV) in young (*A*) and old (*B*) muscle fibers. Experiments were done after blocking calcium conductance with 2 mM Co^{2+}. *A-B* represents the difference between *A* and *B*. Charge movement was computed as the integral of the area underneath the outward current at the beginning and after the end of membrane depolarizations. The maximum charge movement at different potentials in old muscle fibers was significantly less than in young muscle fibers. Figure 2*C* shows the amount of charge movement-membrane potential relationship. Data from young and old muscle fibers were represented in filled and open circles, respectively. As in young fibers, charge movement was recorded at membrane potentials as negative as −70 mV. The charge movement saturated at about 0 mV. The smooth curves were drawn according to the best fit of the average values to a Boltzmann relation of the form: $Q = Q_{max}/(1 + \exp(V_{1/2} - V/k))$, where Q_{max} is the maximum charge moved, $V_{1/2}$ is the midpoint potential of the curve,

Table 1. Passive electrical properties

Age groups	d (μm)	IC (nF)	C_m ($\mu F/cm^2$)	R_m $\Omega \cdot cm^2$	R_i $\Omega \cdot cm$	$r_e/(r_e + r_i)$
25–35	53.7 (2.9)	5.58 (0.30)	10.4 (0.95)	6355 (1154)	367 (17)	0.974 (0.011)
65–75	34.0 (2.3) (*)	3.13 (0.57) (*)	11.3 (0.95)	6123 (1123)	418 (59)	0.992 (0.041)

The variables are: d = fiber diameter; IC = input capacitance; C_m = specific membrane capacity; R_m = specific membrane resistance; R_i = specific internal resistance; $r_e/(r_e + r_i)$ = ratio between external resistance (r_e) and the sum of r_e and the internal resistance (r_i) per unit length. Values in parentheses are means ± SEM (*) = $P < 0.05$ (Student t-test, unpaired data).

and k is the steepness of the curve. The best fit of the data gave the following values for young fibers: Q_{max} = 7.6 nC/μF, $V_{1/2}$ = −31.9 mV and k = 14.0 mV (n = 36). Values of the fitting in old fibers were: Q_{max} = 3.6 nC/μF, $V_{1/2}$ = −28.8 mV and k = 15.2 mV (n = 39). In summary, despite significant differences in the amount of charge moved at different potentials, the voltage dependence or charge distribution did not change.

The possibility that during the biopsy procedure voltage sensors are inactivated as a consequence of the muscle mechanical disruption was tested. To this end, we explored potential differences in charge 1 and charge 2 distribution in both groups. Fibers were voltage-clamped at a holding potential of −90 or 0 mV and pulsed toward more positive or negative potentials. Figure 3*A* shows charge movement traces in fibers from young (*A-C*) and old (*C-D*) muscles. Traces in *A* and *C* were obtained by pulsing the cell from a holding potential of −90 to 0 mV for 100 msec. Subsequently, the holding potential was changed to 0 mV for 3 sec. A pulse to +100 mV was used as a control to subtract linear capacitive current from records obtained with pulses of different amplitude (−20 to −220 mV). Figure 3*B–D* illustrates pulses to −180 mV. As shown in Fig. 2, it is unlikely to move charge 1 at potentials more negative than −100 mV (Brum, Ríos & Stefani, 1988). Figure 3*E* shows the charge distribution for fibers from young and old muscles. Although, in these experimental conditions the time integral of the intramembrane currents had negative values, we used their absolute value. In this way, experimental points and the fitted curve were plotted in the same region for polarized fibers (*see* Fig. 2) instead of lying in the negative region (Caputo & Bolaños, 1989). The best fit of the average values to a Boltzmann relation was drawn as explained for charge 1 (*see above*). The best fit of the data gave the following values for young fibers: Q_{max} = 7.4 nC/μF, $V_{1/2}$ = −78.2 mV and k = 35.6 mV (n = 10). Values of the fitting in old fibers were: Q_{max} = 3.3 nC/μF, $V_{1/2}$ = −81.0 mV and k = 34.2 mV (n = 10). As reported for amphibian fibers, membrane depolarization affects the voltage dependence of charge movement, causing a shift of the Q-V relationship toward more negative potentials and a decrease in the curve

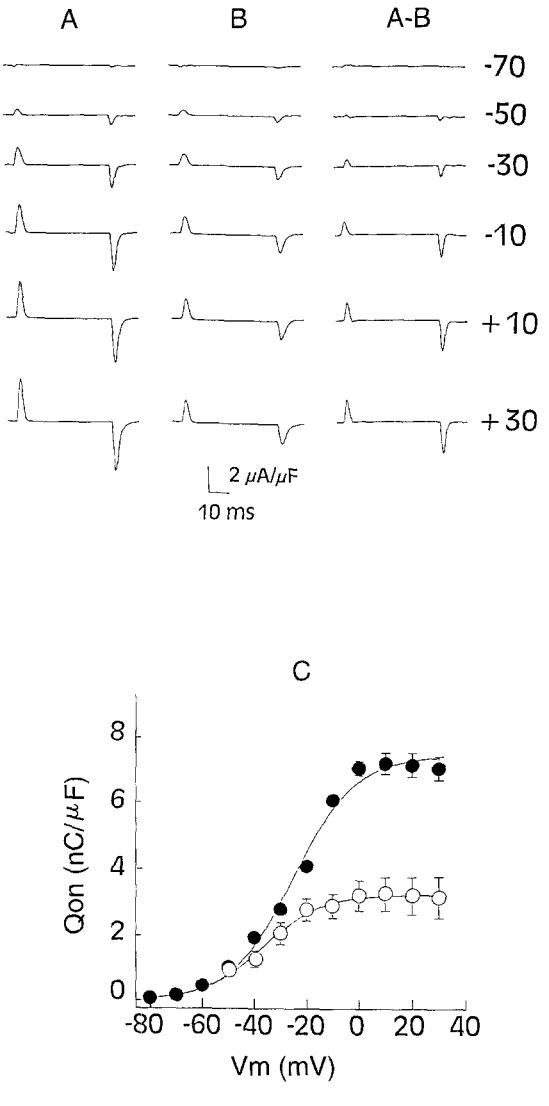

Fig. 2. Charge movement recorded under voltage clamp at different potentials (from −70 to +30 mV) in young (*A*) and old (*B*) muscle fibers after blocking calcium conductance with 2 mM Co^{2+}. *A-B* represents the difference between *A* and *B*. For the calculations of charge movement see text. *C* shows the charge movement-membrane potential relationship. Data from young and old muscle fibers are represented in filled and open circles, respectively. The smooth curves were drawn according to the best fit of the average values to a Boltzmann relation.

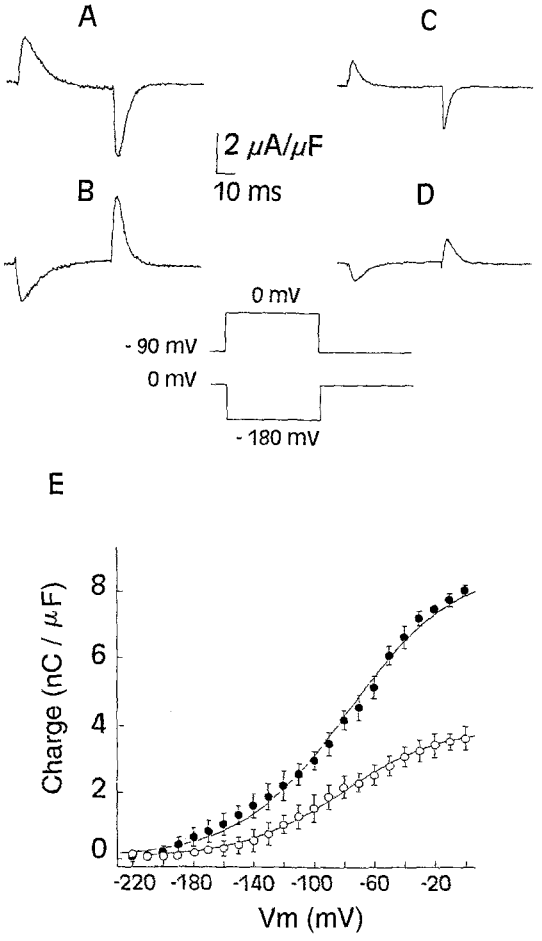

Fig. 3. Charge movement at two holding potentials (V_h = –90 and 0 mV). Charge movement in the depolarizing direction is plotted in Fig. 2. Fibers at V_h = –90 and pulsed toward more positive potentials for 100 msec are illustrated in *A* and *C* for young and old fibers, respectively. Fibers at V_h = 0 mV and pulsed toward negative potentials are illustrated in *B* and *D* for young and old fibers, respectively. Panel *E* shows the charge distribution for fibers from young (filled circles) and old muscles (open circles). The mean of the experimental points were fitted to a Boltzmann relation.

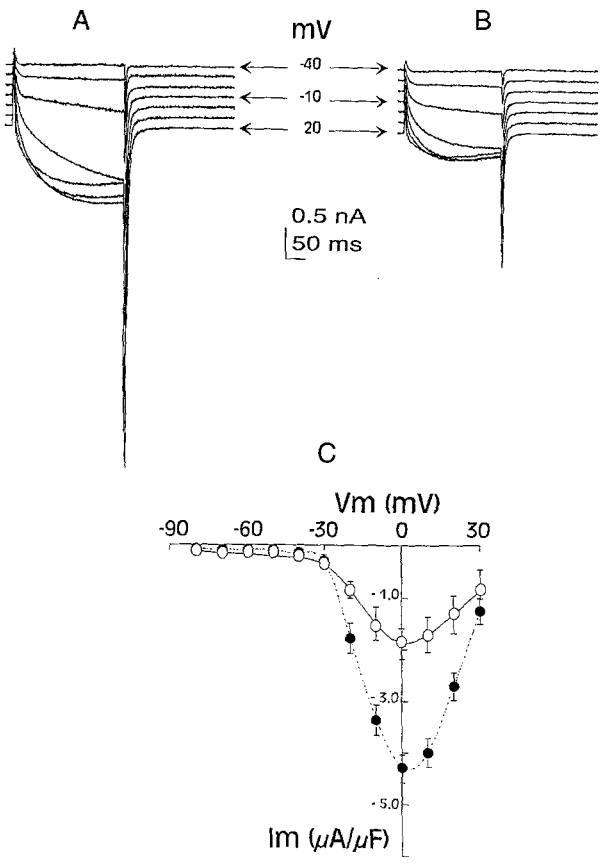

Fig. 4. I_{Ca} records in young and old muscle fibers. I_{Ca} for young (*A*) and old (*B*) fibers are illustrated in the –40 to +20 mV voltage range. An offset was imposed to separate and better identify the traces. (*C*) Current-voltage relationship obtained from experiments as those shown in *A* and *B*. Filled circles and discontinuous line correspond to experiments in young muscle fibers. Open circles and continuous line correspond to data from aged muscles. The mean I_{Ca} amplitude was fitted to a Goldman-Katz equation (*see* text).

steepness (Caputo & Bolaños, 1989). Data from polarized and depolarized fibers demonstrate that the amount of total charge did not differ significantly. The main conclusion from these experiments is that the charge distribution for young and old fibers is similar, and the maximum charge difference in polarized and depolarized fibers is similar for both groups. To test potential effects of the biopsy procedure on charge movement, we also compared our results with data published on human muscle obtained by surgical biopsies (*see* Discussion).

Another way to explore functional alterations of the DHPR in older muscle fibers was to measure the amplitude and voltage-dependence of the dihydropyridine-sensitive calcium current. Figure 4 shows that I_{Ca} amplitude in old muscle fibers was smaller than in younger fibers. The fact that I_{Ca} was affected by agonist (BAY K8644, 1 μM) and antagonist (nifedipine, 0.5 μM) dihydropyridines, supports that the L-type Ca^{2+} channel is the ionic channel responsible for calcium ion conductance (*data not shown*). Figure 4 shows calcium current traces at different voltages in young (*A*) and old (*B*) groups. Currents from –40 to +20 mV are shown with an imposed offset to separate and identify the traces more clearly. Pulses to –40 do not elicit I_{Ca} and only charge movement traces are seen. I_{Ca} is activated at –30 mV reaching the maximum amplitude at 0 mV. Differences in I_{Ca} amplitude between both groups are evident during depolarization and immediately after repolarization in the I_{Ca} tail currents. Figure 4*C* shows the current-voltage relationship for both groups. Filled circles and the discontinuous line correspond to experiments in young muscle fibers. Open circles and the continuous line correspond to the data from older muscles. There was a significant difference ($P < 0.01$) comparing I_{Ca} ampli-

tudes from −20 to +20 mV. The peak I_{Ca} amplitude was −4.7 μA/μF ±0.08 and −2.15 ± 0.11 μA/μF, for young and old fibers, respectively. The mean I_{Ca} amplitude was fitted to the Goldman-Katz function: $I_{Ca} = (1/(1 + \exp((V_{1/2} - V)/k))) ((4F^2VP_{Ca}[Ca^{2+}]_o (\exp(2F(V - V_{Ca})/RT) - 1))/(RT[(\exp(2FV/RT) - 1)]))$, where F, R and T have the usual thermodynamic meanings; k is the slope of the curve, $V_{1/2}$ is the half activation potential, and V_{Ca} is the reversal potential. The first term of this equation corresponds to a Boltzmann relation of the activation form, while the second one is the Goldman-Katz equation. The smooth curves in the graph were drawn according to this fitting. The curves had a similar voltage dependency and half activation potential with $k = 7.3$ and 7.1 mV for young and old fibers, respectively. The $V_{1/2}$ was 2.3 and 1.2 mV for young and old fibers, respectively. This indicates that the effective charge of the Ca^{2+} channel is not modified in old EDL muscles.

A key issue is whether atrophy explains entirely the decline in muscle performance with aging. Normalization of muscle tension per muscle or fiber cross-sectional area demonstrated that a reduction of about 20% in maximum tension cannot be explained by atrophy (*see* Discussion). Therefore, studies on the intrinsic electrical properties of the fiber were performed. Changes in the sarcolemmal surface and intrinsic properties may be responsible for alterations in the ability to voltage-clamp the muscle fiber or for changes in voltage-gated calcium channels density in the tubular sarcolemma. The Table summarizes the sarcolemmal passive properties studied in young and old fibers. Data on membrane capacitance were used for gating and ionic currents normalization. In this way, currents recorded in different fibers were comparable. The following passive fiber properties were determined: (i) fiber diameter (d), (ii) input capacitance (IC), (iii) specific membrane capacity (C_m), (iv) specific membrane resistance (R_m), specific internal resistance (R_i) and $r_e/(r_e + r_i)$ ratio between external resistance (r_e) and the sum of r_e and the internal resistance (r_i) per unit length, according to Delbono (1992). Fibers from the 65–75 group showed smaller diameter and lower input capacitance as a consequence of the lesser contribution of the t-tubule system to the total sarcolemmal area (*see* Discussion). Gating and ionic currents are normalized per membrane capacity or expressed as current densities allowing an accurate estimation of charge and I_{Ca} densities and a comparison between fibers of different groups.

Sarcoplasmic Reticulum (SR) Calcium Release in Aged Muscle Fibers

The following experiments were designed to address whether alterations in the SR calcium release is mediated by uncoupled SR calcium release channels to DHPRs and/or SR calcium depletion.

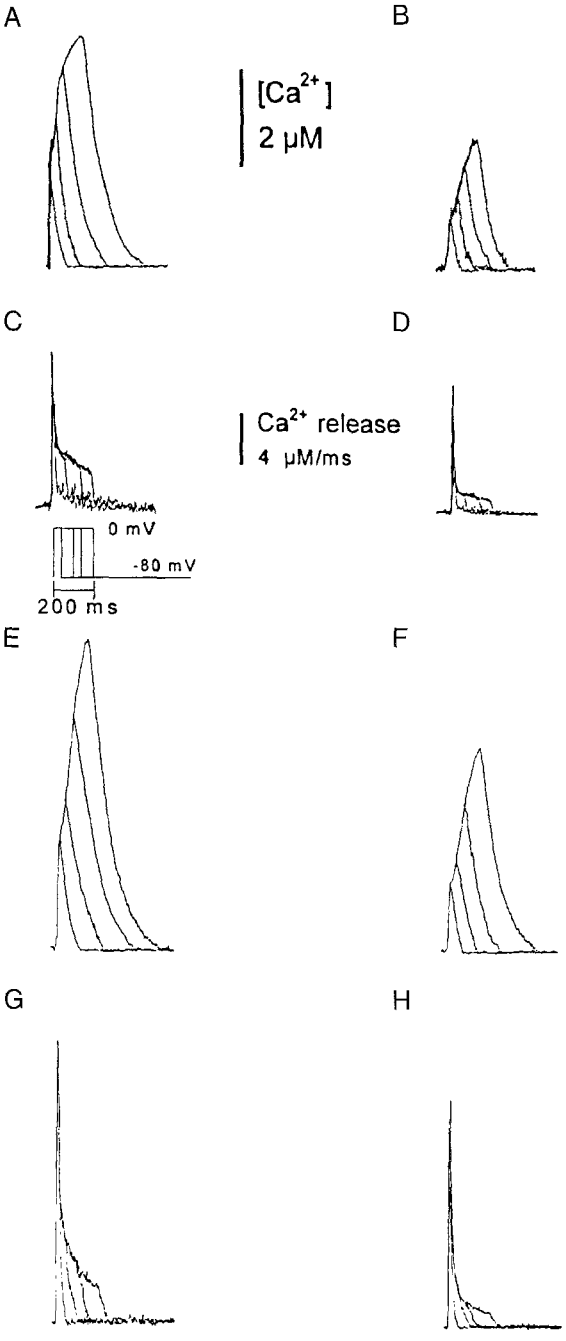

Fig. 5. Ca^{2+} transients with different pulse durations (30 to 200 msec) (*see* pulse protocol) in muscle fibers from the young (*A*) and old (*B*) groups. Their corresponding calculated Ca^{2+} release are illustrated in *C* and *D*. The effect of 0.5 mM caffeine on calcium transients (*E* and *F*) and SR calcium release (*G* and *H*), were recorded in the same fibers illustrated in *A* and *D*. Ca^{2+} transients were monitored with 400 μM mag-fura-2.

Alterations in DHPRs function results in a lower contribution of the DHPR-controlled calcium release to the total calculated calcium release. Figure 5 shows Ca^{2+} transients and Ca^{2+} release with different pulse durations (30 to 200 msec) in muscle fibers from the 25–35 (*A* and

C) and 65–75 (*B* and *D*) groups. Ca^{2+} transients were recorded every 2 min to allow the fiber to return to prestimulation calcium concentrations. Impermeable mag-fura-2 (400 μM) was used as the fluorescent calcium-sensitive dye and a UV-enhanced photodiode as a photodetector following procedures already described (Delbono & Stefani, 1993). Calcium transients were smaller in fibers from older muscles. Peak calcium transients were 6.3 ± 0.4 μM and 4.2 ± 0.3 μM in young and old muscles fibers ($P < 0.01$). The first few milliseconds of the calcium transients express SR calcium release as a single process. After that, the participation of calcium binding proteins and the SR calcium pump are involved in myoplasmic calcium removal. Methods already described were used to study the contribution of the DHPR-controlled and the Ca-controlled calcium release to the total amount of measured SR calcium release (Jacquemond et al., 1991). The total amount of calcium release and its time course were obtained by fitting the Ca^{2+} transients decaying phase to a differential equation describing the myoplasmic calcium removal process, according to Melzer et al. (1986) (*see* Materials and Methods). The peak calcium release or inactivable component represents the calcium-activated calcium release, while the "steady state phase" the noninactivable or voltage-activated calcium release (Jacquemond et al., 1991; Anderson, Cohn & Meissner, 1994; Delbono, 1995). The ratio between the steady-state and the peak calcium release phases represents the amount of coupled DHPR-RyR1 receptors. The steady-state value was measured 100 msec after the beginning of the pulse. Ratios were 0.42 ± 0.05 and 0.18 ± 0.04 for young and old muscle fibers, respectively ($P < 0.01$). In summary, the SR calcium release component under DHPR control is significantly reduced in old skeletal muscle fibers.

As shown in the previous paragraph, after the peak calcium release inactivation, follows a second smaller phase. To determine whether the smaller steady-state phase in fibers from the older group was due to SR calcium content depletion, caffeine was used to potentiate SR calcium release. Caffeine induces SR calcium release without sarcolemmal depolarization. A submaximal caffeine concentration was used to potentiate the calcium-gated SR calcium release. Higher caffeine concentrations are difficult to wash out and, postcaffeine controls for checking fiber injury during the drug exposure, used to be hard to accomplish. In addition, high caffeine induces strong mechanical distortion resulting in inaccurate fluorescent measurements. At low concentrations (0.5 mM), caffeine potentiates calcium release unless the SR is depleted of calcium. Therefore, if an extra amount of calcium is released by caffeine, difference in the peak calcium release cannot be, obviously, attributed to SR calcium depletion.

Figure 5 shows calcium transients and calculated calcium releases elicited by voltage pulses from −80 to 0 mV and 30–200 msec duration in the same fibers from young (*E-G*) and old (*F-H*) muscle fibers shown above (*A-D*). Caffeine was added from a stock (100 mM) to the external solution. The solution in the central pool was replaced completely. An increment in 24.2 ± 3.7% (n = 25) and 23.5 ± 4.6% (n = 23) ($P < 0.01$) in young and old fibers, respectively, was detected in the presence of caffeine. The peak calcium transients were 7.3 ± 0.9 μM and 5.2 ± 1.3 μM ($P < 0.01$) in young and old muscles fibers, respectively.

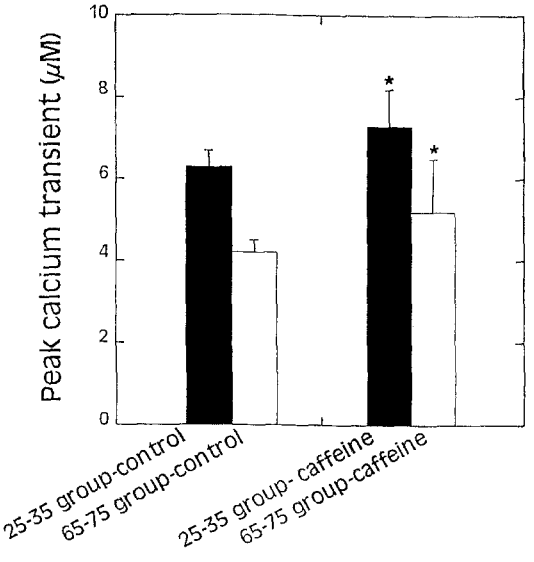

Fig. 6. Effect of caffeine on young and old muscle fibers. Peak calcium transients in 0 caffeine (control) and 0.5 mM caffeine are illustrated in filled and empty bars for the young and older groups, respectively. Asterisks mark statistically significant differences ($P < 0.01$).

Figure 6 shows, comparatively, peak calcium transients and their increments induced by caffeine in each group of fibers. As mentioned above, caffeine activates a voltage-independent component of the SR calcium release through a direct action on the SR calcium release channel/ryanodine receptor. After exposure to caffeine, fibers from both groups maintained the same difference in calcium transient amplitude and both groups of fibers depict a calcium release potentiation.

In summary, residual SR calcium is available in older muscles fibers to be released through a calcium-dependent mechanism. Therefore, differences in calcium release ratios are a consequence of alterations in the DHPR-dependent calcium release mechanism.

Discussion

The main finding of this work is a decrease in skeletal muscle DHPR activity in fast-twitch fibers in the elderly. This alteration partially suppresses one of the mechanisms of SR calcium release. This mechanism involves sarcolemmal voltage sensing followed by increases in

myoplasmic calcium concentration. The calcium increment is amplified secondarily in response to a calcium-gated calcium release mechanism. Thus, the DHPR plays a central role in excitation-calcium release-contraction coupling in skeletal muscle (Tanabe et al., 1987, 1988). Alterations in the DHPR function and/or number might be responsible for decreases in SR calcium release. Decreases in calcium available to trigger muscle contraction may account for reduction in muscle strength with age.

Skeletal Muscle Contractility, Denervation and Relevance of Studies at the Cellular Level in the Elderly

Physically trained people over age 65 maintaining high muscle activity show a decline in mechanical performance tests (Brooks & Faulkner, 1993*a,b*), suggesting that an irreversible component of muscle power decline exists in the elderly. Studies on fast- and slow-twitch skeletal muscle contractility in young and old rats demonstrated changes that can be explained by partial denervation. The tetanic tension is well sustained in slow muscles and decays in fast-twitch muscles from old rats (Edstrom & Larsson, 1987). Similar changes in fast muscle contraction have been reported after chronic denervation (Dulhunty & Gage, 1983, 1985; Obejero Paz, Delbono & Muchnik, 1986; Kotsias & Muchnik, 1987). Alterations in the mechanism of calcium-gated calcium release have been described. Changes in the calcium release channel activity dependent on calcium account for different patterns of muscle contractility after denervation (Delbono & Chu, 1995). The similarity between old and denervated muscles' mechanical performance raises the issue about the contribution of denervated fibers to contraction studies in aged animals. Since it is feasible to define denervation at the single fiber level (Delbono, 1992), it is possible to determine whether alterations in muscle mechanical responses in aged muscles are a consequence of an heterogenous fiber population (innervated and denervated). Slow and denervated fibers were not included in this study. Thus, the alterations in the excitation-calcium release process described in this study occur in fast-twitch fibers. These alterations can account for the mechanical performance impairment in the elderly. Coadjuvant factors might be fiber atrophy and changes in muscle fiber-type distribution.

Decreases in Charge Movement and I_{Ca} in Older Muscle Fibers

The reduction of contractile proteins has its own impact in muscle tension development. The aim of this section is to discuss the involvement of the DHPR independently of muscle fiber atrophy. Skeletal muscle fiber atrophy in the elderly is reflected in a significant smaller diameter (*see* Table). Fibers with smaller diameter have lower capacitance because of the smaller contribution of the sarcotubular membrane (Hodgkin & Nakajima, 1972). The study of the passive membrane properties shows a reduction of the input capacitance in fibers from the 65–75 group. This facilitates the voltage-clamping of the tubular sarcolemmal. However, no proliferation of the t-tubule system was observed, as described for denervated fibers (Delbono, 1992; Delbono & Stefani, 1993), and reflected in the lack of increment in the specific membrane capacity (C_m), in the present work. The absence of sarcolemmal proliferation, together with the presence of a TTX-sensitive sodium current, is another argument against the possibility that fibers included in this study were undergoing a denervatory process. Muscle fiber atrophy is characterized by an absolute decrease in myofilaments content, and little involvement of the membranes system (*see below*). Charge movement and calcium current have been normalized by membrane capacity and expressed as current density to compare determinations from different populations.

We studied potential deleterious effects of the muscle biopsy procedure on cell viability, charge movement inactivation and changes in membrane potential. Fibers were checked for resting membrane potential (V_m) in Ringer-Krebs solution before voltage-clamping. No difference in V_m was detected between groups. V_m values were, -75 ± 6.1 (n = 28) and -77 ± 5.9 (n = 25) for young and old fibers, respectively. To analyze differences in the amount of charge movement between groups, gating currents in polarized and depolarized fibers were studied. No differences in the maximum charge were detected in both experimental conditions. Thus, it is unlikely that the differences described in this work are the consequence of charge immobilization, inactivation or interconversion.

The validity of the needle biopsy procedure to study single muscle fiber physiology is supported by the amount of charge movement recorded in this study *vs.* the values obtained with conventional surgical procedures (García, McKinley & Appel, 1992). Despite using the same recording conditions (voltage-clamp configuration and solutions), García et al. (1992) reported lower maximum charge values than in this work. This suggests that fiber stretching during the biopsy procedure does not alter the voltage sensor.

Decreases in DHPR activity can be explained by: (i) decrease in channel expression, (ii) alterations in DHPR regulation such as phosphorylation by cAMP-dependent protein kinase or protein kinase C (Ma et al., 1992; Sculptoreanu et al., 1993). This point will be elucidated with high-affinity binding and specific antibodies studies together with reconstitution of purified phosphorylated and nonphosphorylated t-tubule membranes. Some recent information provide support to some speculations.

An early reaction to inactive young skeletal muscles is an elevated production of insulin-like growth factor-1 (IGF1) (Caroni & Schneider, 1994). Trophic factors stimulation are associated with induction of c-*fos* and c-*jun* mRNAs production, what is required for sustained enhancement of calcium current (Cavalié et al., 1994). It can be theorized that the decrease in physical activity associated with age is not followed by an increased endocrine/paracrine IGF1 production and/or IGF1R response, what impact negatively in calcium channels expression.

Calcium Current Amplitude and its Relevance in Muscle Contractility

During single twitches the participation of the slow calcium current does not seems to be prominent. Most of the daily activities require the sustained participation of groups of skeletal muscles. Under prolonged stimulation the role of the calcium influx through the DHPR becomes evident (Sculptoreanu et al., 1993), as demonstrated in vitro by unsustained tetanic tension in the presence of DHPR blockers (Kotsias et al., 1986). In this work, the experiments were performed at room temperature to better control the leakage current and to preserve the preparation for longer periods. However contraction studies have been done in vivo or close to physiological temperature in vitro. Q_{10} for the calcium current amplitude is 2.4 in rat muscle fibers what suggest that the physiological contribution of the calcium influx through DHPRs should be prominent (Delbono & Stefani, 1993*a*).

The significant reduction of the calcium current in the older group gives support to the idea that the involvement of the initial steps of excitation-calcium release coupling underlies, at least partially, the skeletal muscle impairment in the elderly. However, a simple extrapolation between the main findings of this work and muscle tension studies cannot be established. The main reason for this is that the fiber population studied in this work appears to be the most affected in aging. In addition, denervated fibers have been excluded. Thus, failure of aged skeletal muscle in contraction tests is the consequence of multiple factors such as those discussed in this paper, denervation-reinervation and motor unit remodeling and, the involvement of slow-twitch muscle fibers, among them.

Reduction in SR Calcium Release is Mediated by Uncoupled SR Calcium Release Channel to DHP Receptors

The peak calcium release or inactivable component represents the calcium-activated calcium release, while the "steady-state phase," the noninactivable or voltage-gated calcium release (Hamilton et al., 1989; Jacquemond et al., 1991; Anderson et al., 1994; Delbono, 1995). The steady-state over the peak calcium release ratio calculations indicate that a greater amount of RYR are uncoupled to DHPRs. Differences detected in calcium transient records and reflected in the calcium release values and waveform prompted us to determine whether smaller responses in aged fibers are the result of SR calcium depletion. Caffeine effect in amphibian fibers has been characterized (Klein, Simon & Schneider, 1990) but no reports exist about the effect of this xanthine on living isolated mammalian muscle fibers. Caffeine directly activates the rat calcium release channel reconstituted into lipid bilayer (Delbono & Chu, 1995). Thus, this drug was used to determine whether a residual SR calcium pool exists after reaching the peak calcium release. This was confirmed by a proportional increment in the peak calcium transient in fibers from both groups. A difference in the peak calcium transient amplitude between the younger and older groups persists after treating fibers with caffeine. The peak calcium transient in the older group after caffeine treatment is smaller compared to the younger group before caffeine (90.1 ± 3.3%, Fig. 5 *F* and *A*). This difference can be explained by changes in the calcium release channel modulation or in myosin isoforms expressed in aged muscles. A decreased calcium sensitivity during submaximal isometric contractions in older muscle fibers (Brooks & Faulkner, 1994) has also been reported. In this work, it has been shown that differences in the peak calcium release is not associated with intracellular calcium stores depletion. However, it cannot be ruled out that during prolonged contractions, differences in SR calcium content are relevant. Decreases in SR volume in aged muscles might be responsible for decreases in intracellular calcium content. Unfortunately, morphological studies on SR surface area and volume in aged muscles, are controversial (Fujisawa, 1975; De Coster et al., 1981). An accurate assessment of the SR calcium content requires measurements of its surface area, volume, free calcium concentration and calcium bound to intraorganelle proteins. Reported methods for measuring SR calcium content in amphibian fibers (Melzer et al., 1986) do not seem to be applicable to this preparation, in which the voltage-sensor is altered.

An interesting finding of this work is that a second slower increase in calcium release was not observed, even in fibers from the younger group, as described for rat muscle fibers (Delbono & Stefani, 1993). As discussed previously, the ability to detect a second phase of inactivable calcium release is related to the peak calcium transient. The peak calcium transients in human muscle is about 50% less than in rat fibers (Delbono, 1995).

Reported Alterations in the DHP Receptor in Other Tissues of Aged Animals

Alterations of the DHPR do not seem to be restricted to the skeletal muscle. Alterations in neurons in senile hip-

pocampal neurones (Landfield, 1987; Reynolds & Carlen, 1989; Pitler & Landfield, 1990; Kostyuk et al., 1993), have been reported. Calcium homeostasis and voltage-activated calcium channels in aged neurons (Gibson & Petersen, 1987; Landfield, 1987), and nerve terminal (Smith, 1984), have been reviewed. An interesting aspect of the studies of the DHPR in hippocampal neurons is the presence of repolarization openings (RO) (Thibault, Porter & Landfield, 1993). Ongoing studies do not demonstrate the presence of RO in aged skeletal muscle and the reduction of I_{Ca} overcomes the increased open probability of the channel during fiber depolarization. Studies on DHPR activity during depolarization and repolarization intent to elucidate differences in DHPR control in aged skeletal muscle and central nervous system.

This work was supported by Grant-in-Aid from the American Heart Association (National) and Muscular Dystrophy Association, and National Institutes of Health (2-P60AG18484-06)

References

Anderson, K., Cohn, A.H., Meissner, G. 1994. High-affinity [3H]PN200-110 and [3H]Ryanodine binding to rabbit and frog skeletal muscle. *Am. J. Physiol.* **266:**C462–C466

Bergström, J. 1962. Muscle electrolytes in man. *Scand. J. Clin. Invest. Suppl.* **68:**1–110

Booth, F.W., Weeden, S., Tseng, H. 1993. Effect of aging on human skeletal muscle and motor function. *Med. Sci. Sports Ex.* **26(5):**556–560

Brooks, S.V., Faulkner, J.A. 1988. Contractile properties of skeletal muscles from young, adult and aged mice. *J. Physiol.* **404:**71–82

Brooks, S.V., Faulkner, J.A. 1991. Maximum and sustained power of extensor digitorum longus muscles from young, adult and old mice. *J. Gerontol.* **46:**B28–33

Brooks, S.V., Faulkner, J.A. 1993*a*. Injury to skeletal muscle fibers during contractions: conditions of occurrence and prevention. *Phys. Ther.* **73:**911–921

Brooks, S.V., Faulkner, J.A. 1993*b*. Skeletal muscle weakness in old age: underlying mechanisms. *Med. Sci. Sports Ex.* **26(4):**432–439

Brooks, S.V., Faulkner, J.A. 1994*a*. Skeletal muscle weakness in old age: underlying mechanisms. *Med. Sci. Sports Exerc.* **26:**432

Brooks, S.V., Faulkner, J.A. 1994*b*. Isometric, shortening, and lengthening contractions of muscle fiber segments from adult and old mice. *Am. J. Physiol.* **267:**C507–C513

Brum, G., Ríos, E., Stefani, E. 1988. Effects of extracellular calcium on the calcium movements of excitation contraction coupling in skeletal muscle fibers. *J. Physiol.* **398:**441–473

Campbell, M.J., McComas, A.J., Petito, F. 1973. Physiological changes in ageing muscles. *J. Neurol. Neurosurg. Psychiatry* **36:**74–182

Caputo, C., Bolaños, P. 1989. Effect of D-600 on intramembrane charge movement of polarized and depolarized frog muscle fibers. *J. Gen. Physiol.* **94:**43–64

Carlson, B.M., Faulkner, J.A. 1988. Reinnervation of long-term denervated rat muscle freely grafted into an innervated limb. Exp. Neurol. *Exp. Neurol.* **102:**50

Caroni, P., Schneider, C. 1994. Signaling by insulin-like growth factors in paralyzed skeletal muscle: rapid induction of IGF1 expression in muscle fibers and prevention of interstitial cell proliferation by IGF-BP5 and IGF-BP4. *J. Neurosci.* **14(5):**3378–3388

Cavalié, A., Berninger, B., Haas, C.A., Garcia, D.E., Lindholm, D., Lux, H.D. 1994. Constitative upregulation of calcium channel currents in rat phaeochromocytoma cells: role of c-fos and c-jun. *J. Physiol.* **479:** 11–27

Coggan, A.R., Spina, R.J., King, D.S., Rogers, M.A., Brown Nemeth, P.M., Holloszy, J.O. 1992. Histochemical and enzymatic comparison of the gastrocnemius muscle of young and elderly men and women. *J. Gerontol.* **47:**B71–B76

De Coster, W., De Reuck, J., Sieben, G., Vander Eecken, H. 1981. Early ultrastructural changes in aging rat gastrocnemius muscle: a stereologic study. *Muscle Nerve* **4:**111–116

Delbono, O. 1992. Calcium current activation and charge movement in denervated mammalian skeletal muscle fibres. *J. Physiol.* **451:**187–203

Delbono, O. 1995. Ca^{2+} modulation of sarcoplasmic reticulum Ca^{2+} release in mammalian skeletal muscle fibers. *J. Membrane Biol.* **146:** 91–99

Delbono, O., Chu, A. 1995. Ca^{2+} release channels in denervated skeletal muscles. *Exp. Physiol.* **80:**561–574

Delbono, O., García, J., Appel, S.H., Stefani, E. 1991. Calcium current and charge movement of mammalian muscle: Action of Amyotrophic Lateral Sclerosis immunoglobulins. *J. Physiol.* **444:**723–742

Delbono, O., Stefani, E. 1993*a*. Calcium current inactivation in denervated mammalian skeletal muscle fibres. *J. Physiol.* **460:**173–183

Delbono, O., Stefani, E. 1993*b*. Calcium transients in mammalian skeletal muscle fibers. *J. Physiol.* **463:**689–707

Dulhunty, A.F., Gage, P.W. 1983. Asymmetrical charge movement in slow- and fast-twitch mammalian muscle fibres in normal and paraplegic rats. *J. Physiol.* **341:**213–231

Dulhunty, A.F., Gage, P.W. 1985. Excitation-contraction coupling and charge movement in denervated rat extensor digitorum longus and soleus muscles. *J. Physiol.* **358:**75–89

Edstrom, L., Larsson, L. 1987. Effects of age on contractile and enzyme-histochemical properties of fast- and slow-twitch single motor units in the rat. *J. Physiol.* **392:**129–145

Engel, A., Stonnington, H.H. 1974. Morphological effects of denervation of muscle. *Ann. NY Acad. Sci.* **228:**68–88

Fabiato, A. 1983. Calcium-induced release of calcium from the cardiac sarcoplasmic reticulum. *Am. J. Physiol.* **245:**C1–C14

Fitts, R.H., Troup, J.P., Witzmann, F.A., Holloszy, J.O. 1984. The effect of ageing and exercise on skeletal muscle function. *Mech. Ageing Dev.* **27:**161–172

Francini, F., Stefani, E. 1989. Decay of the slow calcium current in twitch muscle fibers of the frog is influenced by intracellular EGTA. *J. Gen. Physiol.* **94:**953–969

Fujisawa, K. 1975. Some observations on the skeletal musculature of aged rats. Part 2. Fine morphology of diseased muscle fibres. *J. Neurol. Sci.* **24:**447–469

García, J., McKinley, K., Appel, S.H., Stefani, E. 1992. Ca^{2+} current and charge movement in adult single human skeletal muscle fibres. *J. Physiol.* **454:**183–196

García, J., Schneider, M.F. 1993. Calcium transients and calcium release in rat fast-twitch skeletal muscle fibres. *J. Physiol.* **463:**709–728

Gibson, G.E., Petersen, Ch. 1987. Calcium and the Aging nervous system. *Neurobiol. Aging* **8:**329–343

González, A., Ríos, E. 1993. Perchlorate enhances transmission in skeletal muscle excitation-contraction coupling. *J. Gen. Physiol.* **102:**373–421

Grynkiewicz, G., Poenie, M., Tsien, R.Y. 1985. A new generation of

calcium indicators with greatly improved fluorescent properties. *J. Biol. Chem.* **260:**3440–3450

Gutmann, E., Carlson, B.M. 1976. Regeneration and transplantation of muscles in old rats and between young and old rats. *Life Sci.* **18:**109–114

Hamilton, S.L., Mejía Alvarez, R., Fill, M., Hawkes, M.J., Brush, K.L., Schilling, W.P., Stefani, E. 1989. [3H]PN200-110 and [3H]Ryanodine binding and reconstitution of ion channel activity with skeletal muscle membranes. *Anal. Biochem.* **183:**31–41

Heizmann, C.W. 1984. Parvalbumin, an intracellular calcium-binding protein: distribution, properties and possible roles in mammalian cells. *Experientia* **40:**910–921

Hodgkin, A., Nakajima, S. 1972. The effect of diameter on the electrical constants of frog skeletal muscle fibres. *J. Physiol.* **221:**105–120

Jacquemond, V., Kao, J.P.Y., Schneider, M.F. 1991. Voltage-gated and calcium-gated release during depolarization of skeletal muscle fibres. *Biophys. J.* **60:**867–873

Johnson, M.A., Polgar, J., Weightman, D., Appleton, D. 1973. Data on the distribution of fibre types in thirty-six human muscles. An autopsy study. *J. Neurol. Sci.* **18(1):**111–129

Kanda, K., Hashizume, H. 1989. Changes in properties of the medial gastrocnemius motor units in aging. *J. Neurophysiol.* **61:**737–746

Klein, M.G., Simon, B.J., Schneider, M.F. 1990. Effects of caffeine release from the sarcoplasmic reticulum in frog skeletal muscle fibres. *J. Physiol.* **425:**599–626

Kotsias, B.A., Muchnik, S. 1987. Mechanical and electrical properties of denervated rat skeletal muscles. *Exp. Neurol.* **97:**516–528

Kotsias, B.A., Muchnik, S., Obejero Paz, C.A. 1986. Co^{2+}, low Ca^{2+}, and verapamil reduce mechanical activity in rat skeletal muscles. *Am. J. Physiol.* **250:**C40–46

Kostyuk, P., Pronchuk, N., Savchenko, A., Verkhratsky, A. 1993. Calcium currents in aged rat dorsal root ganglion neurones. *J. Physiol.* **461:**467–483

Landfield, P.W. 1987. "Increased calcium-current" hypothesis of brain aging. *Neurobiol. Aging* **8:**346–347

Larsson, L., Edström, L. 1986. Effect of age on enzyme-hystochemical fibre spectra and contractile properties of fast- and slow-twitch skeletal muscles in the rat. *J. Neurol. Sci.* **76:**69–89

Larsson, L., Salviati, G. 1992. A technique for studies of the contractile apparatus in single human muscle fibre segments obtained by percutaneous biopsy. *Acta Physiol. Scand.* **146:**485–495

Lexell, J., Henriksson-Larsen, K.B., Winglad, B., Sjostrom, M. 1983. Distribution of different fiber types in human skeletal muscles: effects of aging studied in whole muscle cross sections. *Muscle and Nerve* **6(8):**588–595

Ma, J., Gutierrez, L.M., Hosey, M.M., Hosey, E. 1992. Dihidropyridine-sensitive skeletal muscle Ca channels in polarized planar bilayers. 3. Effects of phosphorylation by protein kinase C. *Biophys. J.* **63:**639–647

Melzer, W., Ríos, E., Schneider, M.F. 1986. The removal of myoplasmic free calcium following calcium release in frog skeletal muscle. *J. Physiol.* **372:**261–292

Melzer, W., Ríos, E., Schneider, M.F. 1987. A general procedure for determining calcium release in skeletal muscle fibers. *Biophys. J.* **51:**849–863

Obejero Paz, C.A., Delbono, O., Muchnik, S. 1986. Effects of actinomycin D on contractile properties of denervated rat skeletal muscle. *Exp. Neurol.* **94:**509–518

O'Rourke, K.S., Blaivas, M., Ike, R.W. 1994. Utility of needle biopsy in a university rheumatology practice. *J. Rheumatol.* **21:**413–424

Phillips, S.K., Bruce, S.A., Woledge, R.C. 1991. In mice, the muscle weakness due to age is absent during stretching. *J. Physiol.* **437:**63–70

Phillips, S.K., Wiseman, R.W., Woledge, R.C., Kishmerick, M.J. 1993. Neither changes in phosphorus metabolite levels nor myosin isoforms can explain the weakness in aged mouse muscle. *J. Physiol.* **463:**157–167

Pitler, T.A., Landfield, P.W. 1990. Aging-related prolongation of calcium spike duration in rat hippocampal slice neurons. *Brain Res.* **508:**1–6

Reynolds, J.N., and P.L. Carlen. 1989. Diminished calcium currents in aged hippocampal dentate gyrus granule neurones. *Brain Res.* **479:**384–390

Saltin, B., Gollnick, P.D. 1983. Skeletal muscle adaptability: significance for metabolism and performance. *In:* Handbook of Physiology. Skeletal Muscle. American Physiological Society, editor. p. 572. Bethesda, Maryland

Sculptoreanu, A., Scheuer, T., Catterall, W.A. 1993. Voltage-dependent potentiation of L-type Ca^{2+} channels due to phosphorylation by cAMP-dependent protein kinase. *Science* **364:**240–243

Smith, D.O. 1984. Acetylcholine storage, release and leakage at the neuromuscular junction of mature and aged rats. *J. Physiol.* **347:**161–231

Tanabe, T., Beam, K.G., Powell, J.A., Numa, S. 1988. Restoration of excitation-contraction coupling and slow calcium current in dysgenic muscle by dihydropyridine receptor complementary DNA. *Nature* **336:**134–139

Tanabe, T., Takeshima, H., Mikami, A., Flockerzi, V., Takahashi, H., Kangawa, K., Kojima, H., Matsuo, Hirose, T., Numa, S. 1987. Primary structure of the receptor for calcium channel blockers from skeletal muscle. *Nature* **328:**313–318

Thibault, O., Porter, N.M., Landfield, P.W. 1993. Low Ba^{2+} and Ca^{2+} induce a sustained high probability of repolarization openings of L-type Ca^{2+} channels in hippocampal neurons: physiological implications. *Proc. Natl. Acad. Sci. USA* **90:**11792–11796